Title:	Design for punching of prestressed concrete slabs
Authors:	Clément T., Ramos A.P., Fernández Ruiz M., Muttoni A.
Published in:	Structural Concrete
DOI	10.1002/suco.201200028
City, country:	Lausanne, Switzerland
Year of publication:	2012
Type of publication:	Peer reviewed journal article

Please quote as:	Clément T., Ramos A.P., Fernández Ruiz M., Muttoni A., *Design for punching of prestressed concrete slabs*, Structural Concrete, Lausanne, Switzerland, 2012.

DESIGN FOR PUNCHING OF PRESTRESSED CONCRETE SLABS

Thibault Clément, António Pinho Ramos, Miguel Fernández Ruiz and Aurelio Muttoni

ABSTRACT

Prestressing in flat slabs helps in controlling deformations and cracking under service loads and allows reducing the required slab thickness, leading thus to more slender structures and being therefore an economic solution for long spans. However, as a consequence of the limited thickness of these members, punching is typically governing at ultimate limit state. Investigations on the topic of punching shear strength have shown that the presence of prestress in flat slabs has a number of potential beneficial effects, namely the vertical component (force) carried by inclined tendons, the in-plane compression stresses and the bending moments developed near the supported region. The approach provided by codes of practice for punching design in presence of prestressing may however differ significantly. Some neglect the influence of the introduced bending moments due to prestressing and the sections at which deviation forces of the tendons are considered may be located at different distances from the edge of the supported region. In this paper, the influence of prestressing on the punching shear strength of members without shear reinforcement is investigated by using the fundamentals of the Critical Shear Crack Theory. On that basis, and accounting also for 65 tests available in the scientific literature, the suitability and accuracy of a number of design codes, such as Model Code 2010, Eurocode 2 and ACI 318-11, is investigated and compared.

INTRODUCTION

Prestressed flat slabs are extensively used in Europe for small and medium span bridges. They are also a common solution for foundations mats and long span flat slabs in buildings (for spans larger than 10-12 m) as shown in Figure 1. Although simple in appearance, a flat slab system presents a complex load bearing behaviour, especially at slab-column connections where punching resistance is frequently the governing design criterion. Punching failure results from the interaction of shear forces and bending moments near the supported areas, and is typically characterised by brittle failures (particularly associated to large depth and/or large flexural reinforcement ratios). Although punching failure is local (developing at a single slab-column connection), it overloads adjacent columns and can lead to progressive collapses [3]. In recent years, there had been some examples of progressive collapses of this type of structures that originated important material and human losses (see [6,12]).

With respect to the influence of prestressing on the punching shear strength, it has been reported a number of potential beneficial effects on the literature [22,23]:

- the vertical component resulting from inclined tendons near the column (direct transmission of the shear force to the support),

- the presence of compression stresses in the concrete resulting from prestressing, which have been reported to lead to an increase on the punching shear,

- the moments due to the prestressing eccentricity, that in general have opposite sign to those of from gravity loads and, in this case, have also been reported to increase the punching shear strength.

The present work investigates the influence of prestressing on the punching shear strength of flat slabs. To that aim, the Critical Shear Crack Theory is used. This theory provides a mechanical model suitable for investigating shear and punching shear problems and was selected as the state-of-the-art model to ground *fib* Model Code 2010 (MC2010 [4]) punching shear provisions. The results of this theory, following the MC2010 implementation, as well as other codes based on empirical formulations for punching shear design (such as Eurocode 2 [2] or ACI318-11[1]) are compared to a set of 65 tests available in the scientific literature drawing a number of conclusions on the pertinence and accuracy of each approach.

INFLUENCE OF PRESTRESSING ON THE PUNCHING SHEAR OF CONCRETE SLABS

As previously stated, prestressing induces a number of phenomena influencing punching shear strength. In the following, these phenomena will be investigated on the basis of the Critical Shear Crack Theory (CSCT). A detailed description of the fundamentals of this theory and of its implementation on MC2010 has been presented elsewhere [14].

According to the CSCT, the punching shear strength (V_R) depends on the opening (w) and roughness of a critical shear crack developing through the compression strut carrying shear, Figure 2a. Assuming the opening of the critical shear crack to be proportional to the product of the slab rotation times the effective depth of the slab ($w \propto \psi \cdot d$), and that the roughness of the crack is correlated to the maximum size of the aggregates (d_g), the following failure criterion was proposed by Muttoni for average values [11,14] (Figure 2b, refer to average failure criterion):

$$\frac{V_R}{b_0 \cdot d_v \sqrt{f_c}} = \frac{3/4}{1 + 15 \dfrac{\psi \cdot d}{d_g + d_{g0}}} \tag{1}$$

Where f_c refers to the compressive strength on concrete measured on cylinder, d to the effective depth of the member, d_v to the shear-resisting effective depth (accounting for supported area penetration [14]), b_0 to a control perimeter located at $d_v/2$ from the face of the supported area and d_{g0} is a reference aggregate size (equal to 16 mm).

On the basis of this criterion, and accounting for characteristic material properties and safety factors, the following design failure criterion (V_{Rd}) was proposed [11] and recently adopted by MC2010 [14] (Figure 2b, refer to characteristic failure criterion with $\gamma_c = 1.0$):

$$\frac{V_{Rd}}{b_0 \cdot d_v \dfrac{\sqrt{f_{ck}}}{\gamma_c}} = \frac{1}{1.5 + 0.9 \cdot \psi \cdot d \cdot k_{dg}} \leq 0.6 \tag{2}$$

Where f_{ck} refers to the characteristic compressive strength of concrete measured on cylinder, γ_c is the partial safety factor for concrete (typically equal to 1.5) and k_{dg} is a coefficient accounting for the maximum aggregate size whose value can be calculated as:

$$k_{dg} = 32 \text{ [mm]}/(16+d_g) \geq 0.75 \tag{3}$$

Calculation of a failure load can thus be performed by intersecting the actual behaviour of a slab (characterized by its load-rotation behaviour) with the failure criterion (Figure 2c).

For design of prestressed slabs, the influence of the prestressing has to be accounted on the actions and actual behaviour of the slab. With respect to the shear transferred by concrete (V_c), it can be noted that it is reduced by the inclined component (force) of the tendons (refer to Figure 3a):

$$V_c = R - \int_A q \cdot dA - V_P = V_E - V_P \tag{4}$$

Where R refers to the reaction on the supported area, q to the external loads acting on top of the punching cone, V_E to the acting shear force (difference of the previous components) and V_P to the inclined force carried by the tendons intercepted by the punching surface (alternatively, accounting the deviation forces of prestressing on term q and considering $V_P=0$

yields the same results). It can be noted that punching failure occurs when the shear transferred by concrete ($V_c = V_E - V_P$, Eq. (4)) equals the available concrete strength (V_R, Eqs. (1,2)).

With respect to the influence of prestressing on the behaviour of the slab which is governed by the rotation of the slab (ψ), two different phenomena can be observed. The first one relates to the influence of compression normal stresses acting on the slab (Figure 3b) which delay concrete cracking and stiffen the cracked response of concrete. This leads to stiffer load-rotation behaviours than for non-prestressed slabs for the same amount of flexural reinforcement and increases thus the punching shear strength, refer to point B on Figure 3b. It can be noted that for tensile normal stresses (which should not be the case of prestressing), this effect will lead to a softer response and thus to lower punching shear strength (point C on Figure 3b). The second phenomenon on the load-rotation response refers to the eccentricity of the tendons which originate bending moments on the failure region. These moments, when they oppose to those of the external actions, also delay cracking of the concrete and stiffen the overall response of the member (refer to point B' on Figure 3c where, as sign convention, positive moments lead to tension on the top side of the slab). This is the case for typical arrangements of prestressing tendons. In case the moments are of same sign as those of the external actions, a reduction on the punching shear strength will however follow (softer load-rotation behaviour, refer to point C' in Figure 3c)

These observations on the influence of in-plane forces and bending moments on the punching shear strength were already noted by the Fip Recommendations for the Design of Post-Tensioned Slabs and Foundations [20] and other authors [8,22,23] who proposed to use the decompression moment as a suitable parameter to account for the combined influence of moments and normal forces. This is also the approach followed by the CSCT and that has been implemented on MC2010 as it will later be explained.

With respect to the influence of prestressing on the failure criterion, it can potentially influence the shear transfer capacity of concrete in a positive manner (increase of the compression zone carrying shear). For design purposes, however, this influence is usually neglected. This is for instance the approach followed by MC2010, which nevertheless (and as later shown in the paper) leads to sufficiently accurate and safe results when compared to test results.

DESIGN FOR PUNCHING IN PRESTRESSED SLABS

A number of design codes and recommendations are available for punching shear design of prestressed concrete flat slabs. They however present significant differences in their nature (empirical formulations or physical models) and on the treatment of the prestressing effects and their evaluation. In the following two empirical approaches (Eurocode 2 and ACI 318-11), as well as MC2010 (based on the physical model of the CSCT) will be examined in detail and compared to test results.

Eurocode 2 (2004)

The punching shear strength for Eurocode 2 is expressed in Eq. (5). It can be noticed that the vertical component of tendons $V_{p,EC}$ (see Figure 4) is calculated at $2d$ from the border of the column and is taken into account as an action.

$$V_E - V_{p,EC} \leq V_{R,EC} = \left[0.18 \cdot k \cdot \left(100 \cdot \rho \cdot f_c \right)^{1/3} + 0.1 \cdot \sigma_c \right] b_{EC} \cdot d \qquad (5)$$

where:

$k = 1 + \sqrt{\dfrac{200}{d}} \leq 2$ d being in [mm] (size effect factor, to be noted that no limit is considered by some authors [22,23])

$$\rho = \sqrt{\rho_{lx} \cdot \rho_{ly}} \leq 0.02$$

b_{EC} is the control perimeter located at $2d$ from the border of the column (Figure 4).

This expression accounts for the presence of normal stresses but not for the eccentricity of the tendons (moments).

ACI 318 (2011)

The punching strength prediction is expressed according to Eq. (6), which takes into account the vertical component of the tendons $V_{p,ACI}$, calculated at $0.5d$ from the border of the column as an additional strength, contrary to Eurocode 2.

$$V_E \leq V_{R,ACI} = \left[\beta_p \cdot \sqrt{f_c} + 0.3 \cdot \sigma_c \right] b_{ACI} \cdot d + V_{p,ACI} \tag{6}$$

where:

$$\beta_p = \min\left(3.5 ; \frac{40d}{b_{ACI}} + 1.5 \right)$$

b_{ACI} is the control perimeter located at $0.5d$ from the border of the column (Figure 4)

As for Eurocode 2, this expression accounts for normal stresses but not for eccentricity of the tendons. Contrary to Eurocode 2, no size effect factor is accounted.

Model Code 2010

MC2010 [4] incorporates a number of significant changes with respect to previous versions of Model Code (1978, 1990), refer to [14]. This is particularly relevant for shear and punching shear design for members without transverse reinforcement, where instead of previous empirical formulations, design is based on consistent physical theories. For punching shear, the provisions are grounded on the physical model of the CSCT. Another significant innovation in Model Code 2010 with respect to other codes is that it proposes to

perform design based on the Levels-of-Approximation (LoA) approach, see [13,14]. Such an approach consists on improving the accuracy on the estimate of the strength and behaviour of a member by successive refinements on the value of the physical parameters accounted by the design model. This allows performing simple and low time-consuming estimates of the strength for preliminary design (LoA I) and more refined ones (LoA II and following) for tender or executive design as well as for assessment of existing critical structures. Hereby, it is explained the Model Code 2010 approach to take into account the influence of prestressing on punching shear strength at LoA II and III (typical LoA to be used for structures where punching shear strength is governing). To do so, Model Code 2010 approach for slabs without prestress will first be explained. On that basis, the modifications to be considered for prestressed slabs will be detailed.

In a general manner MC2010 proposes to calculate the punching strength of members without transverse reinforcement as detailed in Equation (7):

$$V_E - V_{p,MC} \leq V_{R,MC} = k_\psi \cdot b_{MC} \cdot d \cdot \sqrt{f_c} \tag{7}$$

Where $V_{R,MC}$ is evaluated according to the CSCT failure criterion (refer to Eq. (2)), whose terms are evaluated through the following parameters:

$$k_\psi = \frac{1}{1.5 + 0.9 \cdot \psi \cdot d \cdot k_{dg}} \leq 0.6 \tag{8}$$

With k_{dg} defined in Eq. (3). The vertical component of the tendons $V_{P,MC}$ is calculated at $0.5d$ from the border of the column as well as for the control perimeter b_{MC} (see Figure 4). The rotation at failure (ψ, refer to Eq. (8)) can be evaluated by using the Levels-of-Approximation approach.

Non prestressed slabs

Level of approximation II

If the slab is subjected to vertical forces as shown in Figure 5a, the expression of the rotation can be given by Eq. (9):

$$\psi = 1.5 \frac{r_s}{d} \frac{f_y}{E_s} \left(\frac{m_s}{m_R} \right)^{3/2} \tag{9}$$

where r_s refers to the distance from the axis of the column to the line of contra-flexure of bending moments and is to be evaluated in the x and y directions. For LoA II and for regular slabs, it can be assumed that the zero moment line is located in the directions x and y at about $r_{sx} = 0.22\ell_x$ and $r_{sy} = 0.22\ell_y$ respectively (where ℓ_x and ℓ_y refer to the span lengths at the x

and y directions respectively, Figure 5a). By using the values of r_{sx} and r_{sy} it is possible to determine the width b_s of the support strip (Figure 5b), on which the moments acting near the supported region ($m_{s,x}$ and $m_{s,y}$) have to be evaluated:

$$b_s = 1.5 \sqrt{r_{sx} \cdot r_{sy}} \tag{10}$$

For inner columns without unbalanced moments (case that will later be compared to test results) and at LoA II, m_s can be estimated as equal to $V/8$. With respect to term m_R, it refers to the unitary bending strength (bending strength per unit length), which can be calculated assuming reinforcement yielding at failure.

Level of approximation III

The expression of the rotation given by Eq. (9) can be used by replacing factor 1.5 by 1.2 if the value of r_{sx} and r_{sy} are obtained from an elastic (uncracked) finite element analysis and the strip moments ($m_{s,x}$ and $m_{s,y}$) are calculated as a function of the distribution of the acting moments on the support strip (b_s). This can be performed by integration along the width of

the support strip and at the border of the supported area (Figure 5c) of the acting moments due to external loads (m_V):

$$m_{sx} = \frac{1}{b_s} \int_{-b_s/2}^{+b_s/2} m_{V,x} dy \quad \text{and} \quad m_{sy} = \frac{1}{b_s} \int_{-b_s/2}^{+b_s/2} m_{V,y} dx \tag{11}$$

Prestressed slabs

Level of approximation II

In presence of prestressing (Figure 6a), the rotation can be calculated according to Eq. (12):

$$\psi = 1.5 \frac{r_s}{d} \frac{f_y}{E_s} \left(\frac{m_s - m_P}{m_R - m_P} \right)^{3/2} \tag{12}$$

This equation incorporates the influence of the decompression moment (m_p), which can be calculated as (refer to Figure 7):

$$m_P = n \cdot \left(\frac{h^2}{12(d - h/2)} + e \right) \approx n \cdot \left(\frac{h}{2} - \frac{d}{3} + e \right) \tag{13}$$

where n is the normal force per unit length, h the height of the slab, d the effective depth and e the eccentricity of the normal force from the centre of gravity of the section. It can be noted that this term effectively accounts for the influence of the in-plane forces (n) and of its resulting bending moments (accounted by means of the prestressing eccentricity, e). As sign convention, the decompression moment is considered positive when it leads to compressive stresses on the top side of the slab (usual cases).

At LoA II, the rest of the parameters of Eq. (12) can be calculated in the same manner as for the case without prestressing. With respect to term m_R, it can be calculated assuming that both ordinary and prestressed reinforcement yield at failure.

Level of approximation III

The rotation can be estimated (in an analogous manner as for non prestressed slabs) by replacing coefficient 1.5 of Eq. (12) by 1.2 if:

- Distances r_{sx} and r_{sy} are calculated according to an elastic (uncracked) analysis of the slab performed accounting for all actions including prestressing (refer to m_{V+P} in Figure 6b). It can be noted that for calculation of these parameters, the influence of prestressing is relatively limited and can in many cases be neglected.

- The strip moments (m_{sx} and m_{sy}) are calculated by integration of the moments acting at the support strip. This integrations has to account for all actions except prestressing (refer to m_V Figure 6c) as prestressing effects are already considered on term m_P.

COMPARISON OF TEST RESULTS WITH DESIGN CODES

A large number of tests are available in the scientific literature dealing with slabs subjected to in-plane forces or prestressed [5, 7-10, 15-19,21,22]. In this section, 65 tests are compared to code predictions from Eurocode 2, ACI 318-11 and MC2010 in order to investigate on the suitability of each code. In the following, the strength predicted by the codes (V_{code}) will be compared to the maximum load of the tests (V_R) accounting for the inclined component of prestressing as previously explained:

$V_R = V_E$ for ACI 318-11 (since $V_{P,\text{ACI}}$ is accounted for in the term of the punching shear strength, refer to Eq. (6))

$V_R = V_E - V_{P,EC}$ for Eurocode 2

$V_R = V_E - V_{P,MC}$ for MC2010

The detailed results are shown in Table 1 and Figure 8. With respect to the influence of the different phenomena induced by prestressing, the following observation can be done:

Influence of the vertical component of the tendons

Figure 8a shows the ratio between the maximum load of the test and the strength predicted by the codes as a function of the normalized vertical component of the tendons (V_p/V_R) calculated according to Figure 4a. ACI 318-11 and MC2010 provide a calculation of the vertical component along the control perimeter located at $0.5d$ from the border of the column, whereas Eurocode 2 provides this value at $2d$ from the border of the column. At this latter distance, more tendons are considered in the calculations and the inclination of the tendons can be significantly larger than at $0.5d$. According to test results, Eurocode 2 control perimeter seems to overestimate the vertical component of the tendons particularly for larger values of V_p/V_R (leading thus to unsafe results). The control perimeter located at $0.5d$ seems to give better (trend-free) predictions, particularly for MC2010.

Influence of in-plane stresses

Figure 8b shows the ratio between the maximum load of the test and the strength provided by the code predictions as a function of a normalized in-plane stress (σ_p/f_c). All the investigated codes take into account the influence of the in-plane stress due to prestress on the punching shear strength. The code providing best predictions is MC2010, particularly at LoA III, where no visible trends are observed. In fact, a test performed by Regan [19] is subjected to a tensile stress (σ_p/f_c = -0.12, left hand-side of the diagrams). While ACI 318-11 and Eurocode 2 do not estimate properly the strength for this test, the prediction of MC2010 at LoA III gives an accurate result, showing that using the decompression moment method provides consistent estimates of the punching strength.

Influence of bending moments

Figure 8c shows the influence of the bending moments (due to prestressing eccentricity). It can be noted that both ACI 318-11 and Eurocode 2 significantly increase their scatter on the

strength predictions for increasing values of the normalized eccentricity (e/d). On the contrary, MC2010 shows a trend-free behaviour, with limited scatter over the whole investigated range.

CONCLUSIONS

The present paper investigates the punching shear strength of prestressed slabs and compares several design codes predictions. The main conclusions of the paper are summarized below:

1. Punching shear strength is in general positively influenced by the presence of prestressing. The inclined component (force) of the tendons intersected by the punching failure surface reduces the shear force carried by concrete. Prestressing also induces both in-plane normal forces (compression) and bending moments (opposite to those of external actions) that increase the stiffness of the members, thus reducing crack widths and increasing punching shear strength.

2. Tendon inclination near the supported area is an effective manner to increase punching shear strength. However, only tendons close to the supported area (at a distance lower or equal than $0.5d$ from the border of the column) are to be considered.

3. Using the decompression moment as a parameter to account for the influence of prestressing in flat slabs is an efficient manner to account both for the in-plane forces and bending moments originated by prestressing.

4. Most empirical design models, however, neglect the influence of bending moments due to prestressing. This leads to inaccurate results when compared to test results.

5. ACI 318-11 code provides, on average, safe results with a quite large scatter. Eurocode 2 provides better results on average than ACI, but with still large scatter of results and may lead potentially to fairly unsafe predictions of the punching shear

strength. This is partly motivated by the choice of the perimeter at $2d$, which seems to overestimate the contribution of inclined tendons.

6. The best predictions are obtained with Model Code 2010. Unlike the other investigated codes, Model Code 2010 is the only one that seems to take into account all effects of prestressing (normal in-plane force, tendons eccentricity and tendons inclination). Consequently the results are more accurate and less scattered. Furthermore, this approach seems not to lead to any tendencies as a function of the main physical parameters. Both Level-of-Approximations II and III proposed by the code lead to good estimates, although Level-of-Approximation III provides better results on average and a lower scatter. This latter level requires performing a linear analysis of the moment field of the slab, which is particularly suitable for highly unsymmetrical geometries as prestressed slab bridges.

NOTATIONS

The following symbols are used in this paper:

b_0 control perimeter

b_s length of moment integration

c column size (if squared)

d effective depth

d_v effective depth

d_g maximum aggregate diameter size

e eccentricity of the normal force from the center of gravity of the section

f_c average concrete compressive cylinder strength

h depth of the slab

k_{dg} coefficient depending on the aggregate size

k_ψ coefficient depending on the rotation

m_P average decompression moment over the width b_s per unit length

m_R resisting moment per unit length

m_s average moment over the width b_s per unit length

m_V moment due to actions other than prestressing

m_{V+P} moment due to all actions (including prestressing)

n normal force per unit length

r_c column radius

r_s radius from the center of the column the the zero moment line

x x direction

y y direction

ℓ span of the slab

V shear force

V_R punching shear strength

V_{code} punching shear strength provided by a code

V_p vertical component of the tendons force on a specified section

V_E acting shear force

β_p coefficient depending on the type of column for ACI approach

ϕ column diameter (if circular)

σ_P normal compressive stress

ψ rotation of the slab outside the column region

ψ_R rotation of the slab at failure

$_{ACI}$ related to ACI 318 (2011)

$_{EC}$ related to Eurocode 2 (2004)

$_{MC}$ related to Model Code 2010

REFERENCES

[1]   ACI *Building Code Requirements for Structural Concrete*, ACI 318-11, American Concrete Institute, ACI Committee 318, 503 p., Detroit, 2011.

[2]   Eurocode *Eurocode 2: Design of concrete structures - Part 1-1: General rules and rules for buildings*, European Committee for Standardization (CEN), Brussels, December, 2004.

[3]   Fernández Ruiz, M., Mirzaei Y., Muttoni, A., *Post-Punching Behavior of Flat Slabs*, ACI Structural Journal, accepted for publication

[4]   FIB *fib Model Code 2010 Final Draft*, 653 p., Lausanne, Suisse, March, 2012.

[5]   Hassanzadeh G. *Betongplattor pa pelare Dimensioneringsmetoder för plattor med icke vidhäftande spännarmering*, Institutionen för Byggkonstruktion, Kungl. Tekniska Högskolan, Bulletin 43, 162 p., Stockholm, Sweden, 1998.

[6]   Kaminetzky D. *Design and Construction Failures - Lessons from Forensic Investigations*, McGraw-Hill., New York, 600 p., 1991.

[7]   Kordina K., Nölting D. *Tragfähigkeit durchstanzgefährdeter Stahlbetonplatten*, Deutscher Ausschuss für Stahlbeton, 371, 167 p., Berlin, Germany, 1986.

[8]   Lúcio, V. J. G., Appleton, J. A. S., and Almeida, J. F. *Ultimate limit state of punching in the (fib) FIP recommendations for the design of post-tensioned slabs and foundations*. Structural Concrete, Vol. 1, no. 3, pp.143-149, 2000

[9]   Melges J. L. P. *Analise experimental da punçao em lajes de concreto armado e protendido*, Escola de Engenharia de São Carlos, Universidade de São Paulo, 414, São Carlos, Brazil, 2001.

[10]   Moreillon L. *Poinçonnement de dalles minces en béton à hautes performances*, Ecole d'ingénieurs et d'architectes de Fribourg, 83 p., Suisse, 2008.

[11] Muttoni A. *Punching shear strength of reinforced concrete slabs without transverse reinforcement*, ACI Structural Journal, V. 105, N° 4, pp. 440-450, USA, July-August, 2008.

[12] Muttoni A. *Sécurité structurale des parkings couverts*, Documentation SIA, A. Muttoni, Editor, 105 p., Zürich, Switzerland, June, 2008.

[13] Muttoni A., Fernández Ruiz M. *Levels-of-approximation approach in codes of practice*, Structural Engineering International, 2012 Vol. 2, pp. 190-194, Zurich, Switzerland, May, 2012.

[14] Muttoni A., Fernández Ruiz M. *The levels-of-approximation approach in MC 2010: application to punching shear provisions*, Structural Concrete, Vol. 13, pp. 32-41, 2012.

[15] Nylander H., Kinnunen S., Ingvarsson H. *Genomstansning av pelarunderstödd plattbro av betong med spänd och ospänd armering*, Test Report KTH, nr. 123, 56 p., Stockholm, Sweden, 1977.

[16] Pralong J., Brändli W., Thürlimann B. *Durchstanzersuche an Stahlbeton und Spannbetonplatten*, Birkhäuser Verlag, Institut für Baustatik und Konstruktion ETH Zürich, Nr. 7305-3, Switzerland, 1979.

[17] Ramos A.P. *Punçoamento em lajes fungiformes pré-esforçadas*, Universidade Tecnica de Lisboa - Instituto Superior Tecnico, 292 p., Lisboa, Portugal, 2003.

[18] Ramos, A. P., Lúcio, V e Regan, P.E.. *Punching of flat slabs with in-plane force*, Engineering Structures, Volume 33, Issue 3 , March, 2011.

[19] Regan P. E. *Punching Shear in Prestressed Concrete Slab Bridges*, Engineering Structures Research group, Polytechnic of Central London, 230 p., London, UK, January, 1983.

[20] SETO, Design of Post-Tensioned Slabs and Foundations, FIP Recommendations, London, 1999, 44 pp.

[21] Shehata I. A. E. M. *Theory of punching in RC slabs*, Ph.D Thesis, Polytechnic of Central London, UK, 1985.

[22] Silva R. J. C., Regan P. E., Melo G.S.S.A, *Punching resistances of unbonded post-tensioned slabs by decompression methods*, Thomas Telford and fib, Structural Concrete, No 1, 21 p., 2005.

[23] Silva R. J. C., Regan P. E., Melo G.S.S.A, *Punching of Post-Tensioned Slabs—Tests and Codes*, American Concrete Institute, Vol. 104, No. 2, pp. 123-132, 2007

Corresponding author:

Miguel Fernández Ruiz

Ecole Polytechnique Fédérale de Lausanne - IBETON

Station 18 Lausanne CH-1024

Switzerland

Email: miguel.fernandezruiz@epfl.ch

Figures:
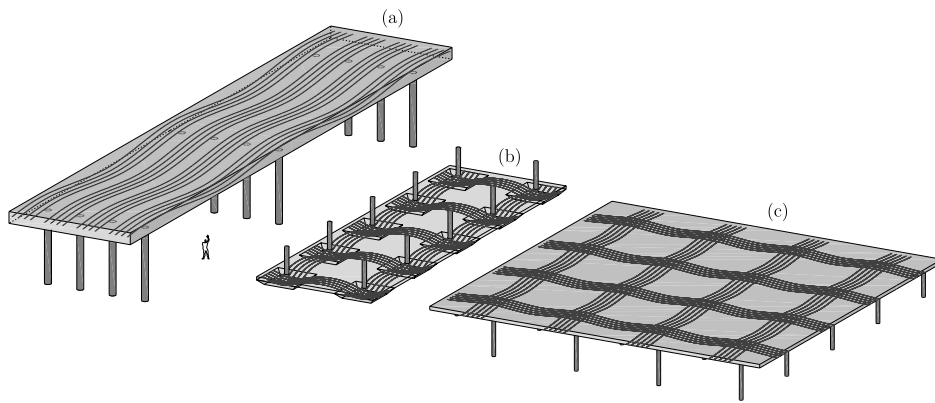
Figure 1:   Examples of prestressed structures: (a) slab bridge; (b) footings; and (c) flat slab
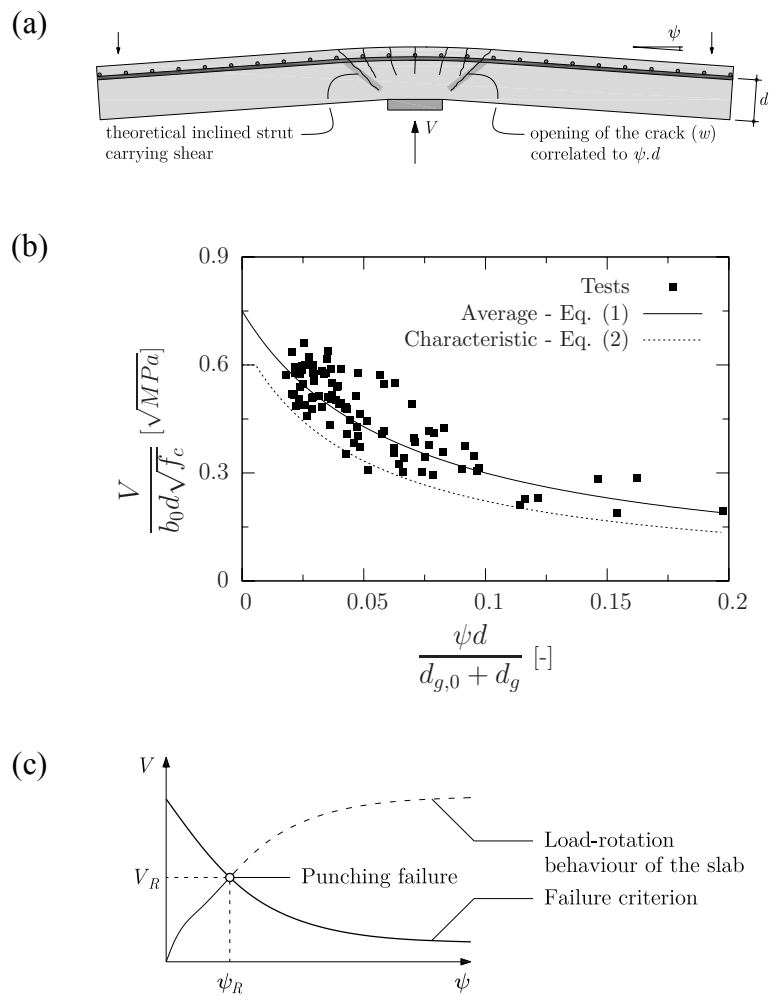
Figure 2:   The Critical Shear Crack Theory: (a) critical shear crack developing through the

compression strut carrying shear; (b) failure criteria and comparison to 99 test results

(data according to [11]); and (c) calculation of the strength and deformation capacity
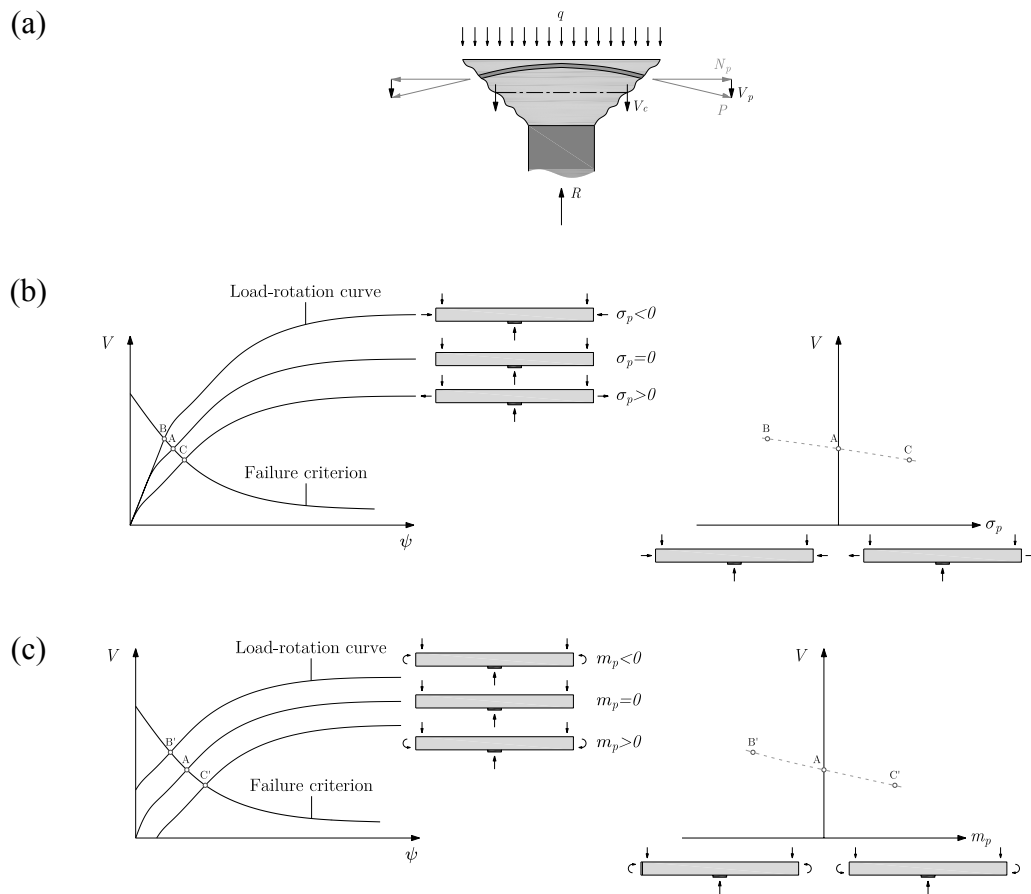
Figure 3:   Phenomena influencing punching shear strength of prestressed slabs: (a) reduction of

shear force due to the inclined component (force) of tendons; (b) influence of an in-

plane force; and (c) influence of a bending moment

1
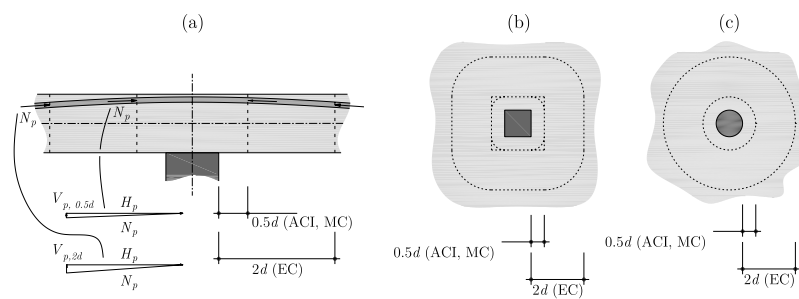
Figure 4:   Parameters of design codes: (a) vertical component of the tendons according to ACI

318, Eurocode 2 and Model; (b) square columns; and (c) circular columns
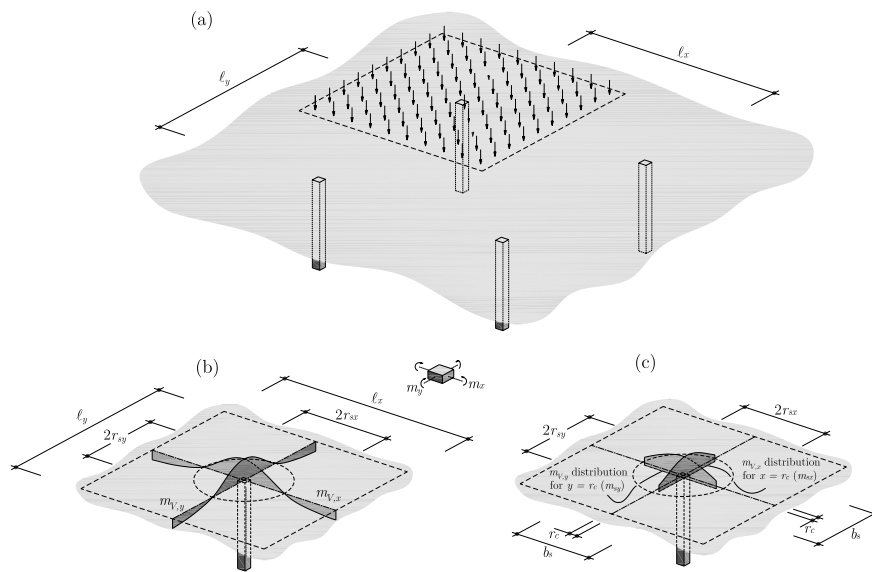
Figure 5:   Non-prestressed flat slab: (a) geometry; (b) moment distribution ($m_{V,x}$, $m_{V,y}$) in each direction over the support; and (c) moment distribution ($m_{V,x}$, $m_{V,y}$) at edge of supported area over a length b_s
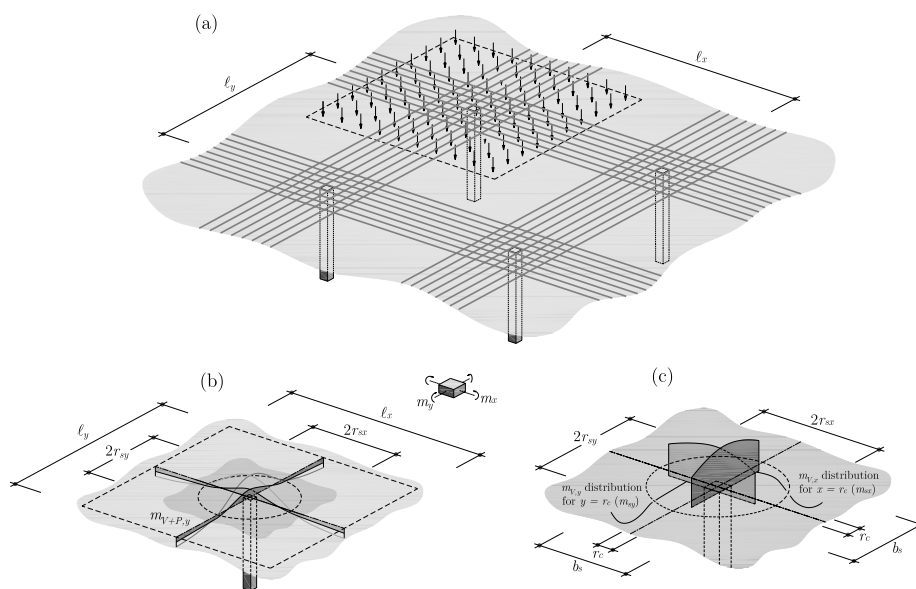
Figure 6:   Prestressed flat slab: (a) geometry; (b) total moment distribution ($m_{V+P,x}$, $m_{V+P,y}$) in each direction over the support; and (c) moment distribution due to actions excluding prestressing ($m_{V,x}$, $m_{V,y}$) at edge of supported area over a length b_s
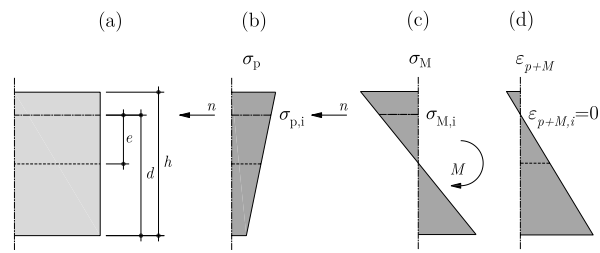
Figure 7:   Decompression moment: (a) Section subjected to in normal force, (b) state of associated stress, (c) state of stress due to decompression moment and (d) resulting state of strain

Figure 8:   Prediction of the punching strength for tests taken from the literature as a function of:

(a) the ratio between the vertical component of the tendons and the strength of the test;

(b) the introduced in-plane compression stress; and (c) the applied moments due to

tendon or i-plane force eccentricity

Table 1: Comparison of test results and investigated codes

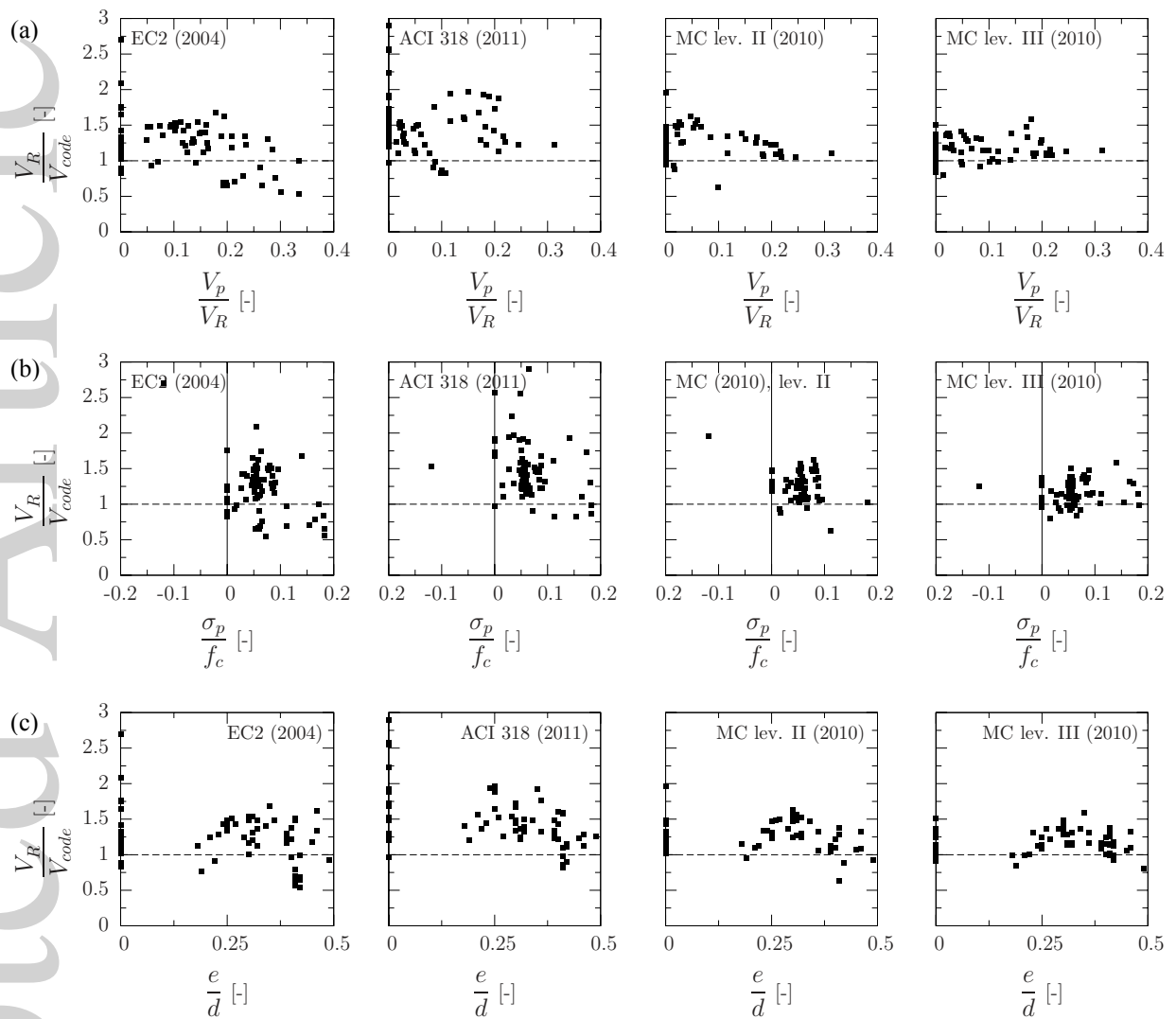| Author	Slab	V_E	$V_{p,0.5d}$	$V_{p,2d}$	d	f_c	σ_p	c or ϕ^{**}	$V_R/V_{R,EC}$	$V_R/V_{R,ACI}$	$V_R/V_{R,MC,II}$	$V_R/V_{R,MC,III}$
		[kN]	[kN]	[kN	[mm]	[MPa]	[MPa]	[mm]	[-]	[-]	[-]	[-]
Kinnunen and al.	Pl1	709	70.3	141	205	35.1	3.93	240 (φ)	0.69	0.82	0.63	1.10
Kinnunen and al.	Pl2	796	70.4	211	204	28.8	5.25	240 (φ)	0.65	0.98	(*)	1.11
Kinnunen and al.	Pl3	920	70.4	211	204	31.9	5.25	240 (φ)	0.79	1.10	(*)	1.27
Kinnunen and al.	Pl4	701	70.4	211	204	28.7	5.25	240 (φ)	0.56	0.86	(*)	0.96
Kinnunen and al.	Pl6	659	70.3	141	205	25.5	3.93	240 (φ)	0.70	0.83	(*)	0.98
Pralong and al.	P5	568	0	0	154	27.1	2.65	300 (φ)	1.08	1.71	1.18	1.02
Pralong and al.	P7	767	106	160	160	31.2	2.60	300 (φ)	1.18	1.23	1.07	1.01
Pralong and al.	P8	683	106	160	158	29.6	3.00	300 (φ)	1.34	1.13	1.09	1.03
Pralong and al.	P9	820	106	160	158	35	2.90	300 (φ)	1.62	1.29	1.33	1.24
Shehata	SP1	988	177	177	130	36.5	5.14	150 (c)	1.68	1.93	(*)	1.59
Shehata	SP2	624	88	88	129	46.4	5.14	150 (c)	0.97	1.61	(*)	1.01
Shehata	SP3	416	0	0	151	41.0	0	150 (c)	0.83	1.92	1.18	1.09
Shehata	SP4	884	177	296	129	41.7	7.20	150 (c)	1.00	1.73	(*)	1.27
Shehata	SP5	780	133	222	129	40.9	3.60	150 (c)	1.16	1.67	1.25	1.33
Regan	DT1	780	0	0	197	43.6	0	150 (c)	1.02	1.73	1.28	1.35
Regan	DT2	832	40.2	161	177	40.1	8.90	150 (c)	0.69	1.15	(*)	1.12
Regan	DT3	962	80.4	322	177	43.2	8.90	300 (c)	0.54	0.90	(*)	0.92
Regan	DT4	715	12.6	50.0	177	47.2	2.80	150 (c)	0.99	1.11	0.88	1.12
Regan	DT6	832	40.2	161	177	42.9	8.90	150 (c)	0.67	1.15	(*)	0.98
Regan	DT8	676	9.90	39.6	184	45.6	2.20	150 (c)	0.93	1.26	0.93	1.17
Regan	DT9	806	40.2	161	177	45.0	8.90	150 (c)	0.65	1.11	(*)	0.94
Regan	DT10	832	40.2	161	177	43.7	8.90	150 (c)	0.65	1.15	(*)	0.98
Regan	BD1	293	0	0	101	42.2	7.65	100 (c)	0.84	1.30	1.02	1.14
Regan	BD2	268	0	0	101	39.2	0	100 (c)	1.76	1.92	1.48	1.30
Regan	BD5	208	0	0	101	33.1	-3.95	100 (c)	2.70	1.53	1.96	1.25
Kordina and al.	V1	450	74.1	74.1	126	33.6	1.70	200 (φ)	1.17	1.26	1.05	0.92
Kordina and al.	V2	525	71.9	71.9	126	36.0	1.66	200 (φ)	1.26	1.48	1.09	0.98
Kordina and al.	V3	570	134	134	124	36.0	3.09	200 (φ)	1.22	1.22	1.10	1.05
Kordina and al.	V6	375	0	0	118	30.4	1.77	200 (φ)	1.33	1.49	1.23	0.99
Kordina and al.	V7	475	77.1	77.1	126	31.2	1.77	200 (φ)	1.25	1.34	1.13	0.99
Kordina and al.	V8	518	77.1	77.1	126	35.2	1.77	200 (φ)	1.38	1.43	1.22	1.07
Hassanzadeh	A1	668	75	184	151	31.0	2.79	250 (φ)	1.30	1.23	1.05	1.07
Hassanzadeh	A2	564	0	59.0	146	28.7	2.74	250 (φ)	1.49	1.32	1.06	1.05
Hassanzadeh	B1	439	0	0	190	40.9	0	250 (φ)	0.89	0.97	1.21	1.07
Hassanzadeh	B2	827	0	0	190	39.0	2.12	250 (φ)	2.09	1.92	1.43	1.49
Hassanzadeh	B3	1113	74	178	190	38.6	2.21	250 (φ)	1.51	1.59	1.38	1.40
Hassanzadeh	B4	952	0	52.6	190	40.5	1.99	250 (φ)	1.48	1.58	1.29	1.25

Author	Slab	V_R [kN]	$V_{p,0.5d}$ [kN]	$V_{p,2d}$ [kN]	d [mm]	f_c [MPa]	σ_p [MPa]	c or ϕ^{**} [mm]	V_R/V_{EC} [-]	V_R/V_{ACI} [-]	$V_R/V_{MC,II}$ [-]	$V_R/V_{MC,III}$ [-]
Melges	M1	441	0	0	127	26.6	0	180 (c)	1.20	1.89	1.32	1.13
Melges	M4	772	66	99	132	51.9	2.58	180 (c)	1.49	1.76	1.30	1.24
Moreillon	B1-01	262	0	0	90	90	0	120 (ϕ)	1.25	2.57	1.47	0.96
Moreillon	B1-02	294	0	0	81	90	2.88	120 (ϕ)	1.42	2.23	1.25	0.95
Moreillon	B1-03	330	0	0	76	90	4.33	120 (ϕ)	1.65	2.55	1.23	0.99
Moreillon	B1-04	376	0	0	76	90	5.77	120 (ϕ)	1.75	2.90	1.32	1.10
Ramos	AR2	258	0	0	80	39.1	0	200 (c)	1.24	1.68	1.22	0.99
Ramos	AR3	270	0	0	80	37.5	1.00	200 (c)	1.23	1.49	1.19	1.02
Ramos	AR4	252	0	0	80	43.1	1.55	200 (c)	1.06	1.29	1.05	0.91
Ramos	AR5	251	0	0	80	35.7	2.00	200 (c)	1.09	1.21	1.07	0.95
Ramos	AR6	250	0	0	80	37.0	1.95	200 (c)	1.08	1.21	1.03	0.92
Ramos	AR7	288	0	0	80	43.9	2.75	200 (c)	1.13	1.26	1.10	1.01
Ramos	AR8	380	72.2	72.2	78	41.6	1.95	200 (c)	1.34	1.90	1.25	1.07
Ramos	AR10	371	56.4	56.4	78	41.4	1.51	200 (c)	1.40	1.97	1.31	1.10
Ramos	AR11	342	40.1	40.1	78	38.0	1.04	200 (c)	1.43	1.94	1.34	1.09
Ramos	AR12	280	32.8	32.8	75	31.3	1.95	200 (c)	1.25	1.56	1.10	0.96
Ramos	AR13	261	0	68.2	76	32.5	1.94	200 (c)	0.91	1.37	1.13	0.98
Ramos	AR14	208	0	60.5	76	28.2	1.87	200 (c)	0.76	1.20	0.95	0.82
Ramos	AR15	262	0	32.7	76	31.7	1.93	200 (c)	1.12	1.41	1.15	1.00
Ramos	AR16	351	73.4	73.4	77	30.6	1.92	200 (c)	1.34	1.88	1.23	1.05
Silva	A1	380	8.20	50.8	109	37.8	3.31	100 (c)	1.25	1.54	1.37	1.29
Silva	A2	315	9.00	48.9	113	37.8	2.14	100 (c)	1.12	1.39	1.25	1.09
Silva	A3	353	0	17.4	109	37.8	3.16	100 (c)	1.29	1.45	1.34	1.23
Silva	A4	321	0	16.4	104	37.8	1.98	100 (c)	1.48	1.64	1.47	1.25
Silva	B1	582	30.5	92.5	114	40.1	3.39	200 (c)	1.40	1.49	1.47	1.30
Silva	B2	488	27.3	61.8	110	40.1	2.23	200 (c)	1.49	1.50	1.52	1.25
Silva	B3	520	11.5	48.7	108	40.1	3.12	200 (c)	1.48	1.47	1.47	1.32
Silva	B4	459	11.5	47.1	106	40.1	2.16	200 (c)	1.53	1.49	1.55	1.30
Silva	C1	720	33.9	104	111	41.6	3.33	300 (c)	1.54	1.45	1.63	1.36
Silva	C2	557	33.6	63.0	105	41.6	2.26	300 (c)	1.54	1.37	1.57	1.23
Silva	C3	637	16.8	61.6	106	41.6	3.48	300 (c)	1.51	1.34	1.54	1.29
Silva	C4	497	14.6	50.9	102	41.6	2.31	300 (c)	1.43	1.26	1.50	1.16
Silva	D1	497	9.7	46.9	111	44.1	3.34	200 (c)	1.51	1.52	1.49	1.30
Silva	D2	385	12.6	40.8	105	44.1	2.23	200 (c)	1.24	1.24	1.27	1.08
Silva	D3	395	0	31.3	106	44.1	2.27	200 (c)	1.36	1.32	1.30	1.08
Silva	D4	531	35.9	72.3	102	44.1	2.22	300 (c)	1.31	1.22	1.38	1.13

									EC	ACI	MC,II	MC,III
Mean									1.23	1.48	1.26	1.16
COV									0.30	0.26	0.17	0.14
5% fractile									0.65	0.90	0.93	0.92

(*) decompression moment m_P is larger than m_s. Calculation of the strength is thus not performed at this Level-of-Approximation

(**) c refers to square columns, where c is the side of the column and ϕ refers to circular columns, where ϕ is the column diameter